Biolubricant production from Indian mustard seed oil through ethyl biodiesel-2G precursor using K2CO3 as heterogeneous catalyst

Déya Regragui, Dg Arina Amira Binti Matlan, Graeme Rapp, Richard Trethowan, Alejandro Montoya, Brice Bouyssière, Emilien Girot, Jean-François Portha, Peter Pratt, Lucie Coniglio

Cleaner Engineering and Technology 21 (2024) 100767

Contents lists available at ScienceDirect

Cleaner Engineering and Technology

journal homepage: www.sciencedirect.com/journal/cleaner-engineering-and-technology

Biolubricant production from Indian mustard seed oil through ethyl biodiesel-2G precursor using K_2CO_3 as heterogeneous catalyst

Déya Regragui [a], Dg Arina Amira Binti Matlan [a], Graeme Rapp [b], Richard Trethowan [b], Alejandro Montoya [c], Brice Bouyssiere [d], Emilien Girot [a], Jean-François Portha [a], Peter Pratt [e], Lucie Coniglio [a,*]

[a] Université de Lorraine - Ecole Nationale Supérieure des Industries Chimiques de Nancy, Laboratoire Réactions et Génie des Procédés UMR CNRS 7274, 1, rue Grandville BP 20451, 54001, Nancy, Cedex, France
[b] The University of Sydney, Plant Breeding Institute, I.A. Watson International Grains Research Centre, PO Box 219, Narrabri, NSW, 2390, Australia
[c] School of Chemical and Biomolecular Engineering, The University of Sydney, NSW, 2006, Australia
[d] Universite de Pau et des Pays de l'Adour, E2S UPPA, CNRS, IPREM, UMR5254, HELIOPARC, 2 Avenue du Président Angot, 64053, Pau, France
[e] Valtris Enterprises France, Z.I. Baleycourt BP 10095, 55103, Verdun, France

ARTICLE INFO

Keywords:
Heterogenous catalysis
Biolubricant
Ethyl biodiesel
Indian mustard seed oil
Green chemistry-based production

ABSTRACT

Biolubricants are sustainable alternatives to mineral lubricants and offer environmental, economic and social benefits, including the possibility of producing bioproducts on-farm. Previous research showed that Indian mustard seed oil (IMSO) could be converted into biolubricants by double transesterification using potassium hydroxide as a homogeneous catalyst. The objective of this work was to study the effectiveness of the heterogeneous catalyst potassium bicarbonate (K_2CO_3) for the conversion of IMSO into biolubricant using an ethyl biodiesel precursor in a double transesterification-based process. The first transesterification reaction aimed to convert IMSO into ethyl biodiesel (IMSOEEs) by conducting the ethanolysis under various operating conditions to optimize the process. The optimal operating conditions obtained were: 78 °C, 1.01 bar, 4 wt% K_2CO_3, ethanol to oil molar ratio of 8, and a reaction time of 60 min (with addition of 25 wt% recycled glycerol at 60 min to improve demixing). The second transesterification reaction converted IMSOEEs into biolubricants through reactive distillation with 2-ethylhexanol (2 EH) under the following optimized operating conditions: 100 °C, 0.05 bar, 4 wt% K_2CO_3, 2 EH to IMSOEEs molar ratio of 4, and a reaction time of 120 min. Both ethyl biodiesel and biolubricant were produced with very satisfactory purity (≥96 wt%), thus meeting the expected functional properties.

1. Introduction

Sustainable industry requires a transition towards economically-feasible and environmentally-friendly biomass conversion technologies, that align with the concepts of biorefinery and circular economy, to generate bioenergy carriers and bioproducts by approaching the zero-discharge goal (Raman et al., 2018; Ubando et al., 2020; Roy et al., 2023). This not only secures the local supply of vital human needs, but also contributes to global stability (Coniglio et al., 2023).

Within this context, an Indian mustard biorefinery has recently been proposed that contributes to a green circular economy as illustrated in Fig. 1a (Chen et al., 2019; Rapp et al., 2020, 2021). In fact, this oleaginous plant can grow easily in hot, dry places (Singh et al., 2018) and avoids competition with food crops, while assisting their growth if used in rotation. Indeed, in addition to phytoremediation, Indian mustard can be used for biofumigation and biofertilization of soils in rotational cropping systems to improve yields while promoting biodiversity. Indian mustard can also be integrated into a biorefinery system creating new circular production chains. For example, stems that may be transformed into a translucent thermoplastic film (Sejati et al., 2023), can also, along with roots, be fed into a biological or thermal cogeneration unit to be

* Corresponding author.
E-mail addresses: deya.regragui7@etu.univ-lorraine.fr (D. Regragui), dg-arina-amira.binti-matlan3@etu.univ-lorraine.fr (D.A.A. Binti Matlan), graeme.rapp@sydney.edu.au (G. Rapp), richard.trethowan@sydney.edu.au (R. Trethowan), alejandro.montoya@sydney.edu.au (A. Montoya), brice.bouyssiere@univ-pau.fr (B. Bouyssiere), emilien.girot@univ-lorraine.fr (E. Girot), jean-francois.portha@univ-lorraine.fr (J.-F. Portha), peter.pratt@valtris.com (P. Pratt), lucie.coniglio@univ-lorraine.fr (L. Coniglio).

https://doi.org/10.1016/j.clet.2024.100767
Received 7 March 2024; Received in revised form 7 May 2024; Accepted 5 June 2024
Available online 8 June 2024

Abbreviations

ALSI	Automatic liquid sampler injector system
AES	Atomic Emission Spectrometry
BET	Brunauer-Emmet-Teller
C16:0	Palmitic acid or Ethyl (or 2-ethylhexyl) palmitate
C18:0	Stearic acid or Ethyl (or 2-ethylhexyl) stearate
C18:1	Oleic (or *cis*-vaccenic) acid or Ethyl (or 2-ethylhexyl) oleate (or *cis*-vaccenate)
C18:2	Linoleic acid or Ethyl (or 2-ethylhexyl) linoleate
C18:3	Linolenic acid or Ethyl (or 2-ethylhexyl) linolenate
C20:1	Gadoleic acid or Ethyl (or 2-ethylhexyl) gadoleate
C22:1	Erucic acid or Ethyl (or 2-ethylhexyl) erucate
C24:0	Lignoceric acid or Ethyl (or 2-ethylhexyl) lignocerate
CAGR	Compound Annual Growth Rate
D[3,2]	Sauter mean diameter
DGs	Diacylglycerides (or diglycerides)
Ethyl C18:1	Ethyl oleate
Ethyl C18:2	Ethyl linoleate
Ethyl C18:3	Ethyl linolenate
$ExpA_k$	Experiment k relative to biofuel production
$ExpB_k$	Experiment k relative to biolubricant production
2 EH	2-ethylhexanol
2 EH C18:1	2-Ethylhexyl oleate
2 EH C18:2	2-Ethylhexyl linoleate
2 EH C18:3	2-Ethylhexyl linolenate
2G	Second generation
FAEEs	Fatty acid ethyl esters
FAMEs	Fatty acid methyl esters
FFAs	Free fatty acids
FID	Flame ionization detector
FIMS	Fine Indian mustard stems
GC	Gas-chromatography
ICP	Inductively coupled plasma
IMSO	Indian mustard seed oil
IMSOEEs	Indian mustard seed oil ethyl esters (ethyl biodiesel)
IMSO2EHEs	Indian mustard seed oil 2-ethylhexyl esters (biolubricant)
IS	Internal standard
$[K_2CO_3]$	Potassium carbonate concentration
LOQ	Limit of quantification
MGs	Monoacylglycerides (or monoglycerides)
MHD	Methyl heptadecanoate
MR	Molar ratio
MS	Mass spectrometry
NEVO	Non-edible vegetable oil
STP	Standard temperature and pressure ($T = 273.15$ K; $P = 10^5$ Pa)
SOO	Synthetic oleic oil
SOOEEs	Synthetic oleic oil ethyl esters (ethyl biodiesel)
SOO2EHEs	Synthetic oleic oil 2-ethylhexyl esters (biolubricant)
TGs	Triacylglycerides (or triglycerides)

transformed into heat, power, biogas, and biofertilizers. The seeds can be used for their oil, while the meal (rich in glucosinolates, protein and fiber) can be used for animal feed after extraction of the glucosinolates, which are of medical, dietary and cosmetic interest and are also valuable as biopesticides (Rapp et al., 2021; Albuquerque et al., 2020). Indian mustard oil, which is not intended for food use, has been successfully converted into ethyl biodiesel-2G (second generation biofuel) and biolubricants using two successive homogeneous alkaline transesterifications, followed by dry purification with Indian mustard stems or Montmorillonite clay, supplemented for biolubricants by bubble washing and vacuum heteroazeotropic distillation (Chen et al., 2019; Rapp et al., 2020, 2021). The two adsorbents (Indian mustard stems and Montmorillonite clay) can then be valorized in a biological or thermal cogeneration unit to provide heat, electricity, biogas or biofertilizers, with the advantage that clay can be reactivated for further dry purification cycles. The excess glycerol produced and the wastewater from the biolubricant bubble-washing can be recycled in a dedicated biodigester (fermenter) to be converted into biohydrogen and bioethanol, the latter feeding the ethyl biodiesel production unit after purification (Fig. 1a; Chen et al., 2019; Rapp et al., 2020, 2021).

Double-transesterification has been chosen as the route for chemically modifying the starting oil (source of triglycerides) to achieve the desired biolubricant usage properties (cold flow properties and thermal-oxidative stability). In addition to offering the flexibility of producing an intermediate bioenergy carrier (ethyl biodiesel), double-transesterification can be carried out under alkaline catalysis (homogeneous or heterogeneous), reducing reaction times and corrosion risks, compared to commonly used estolide formation or epoxidation (Kleinaitė et al., 2014; de Haro et al., 2018; Chan et al., 2018; Rapp et al., 2021). These alternatives are generally carried out under homogeneous acid catalysis, and are less economically favorable (costly reagents are required for estolide formation, and multi-stage reactions take part in epoxidation which must be followed by ring opening and acetylation). Nevertheless, double-transesterification requires high oleic oils to yield biolubricants that fulfill the standards, and the second transesterification step must be carried out under reduced pressure to lower the reaction temperature (Rapp et al., 2021). In addition, while 2-ethylhexanol (2 EH) commonly used to produce biolubricants for metalworking (Zheng et al., 2018) was selected, non-conventional ethyl biodiesel (fatty acid ethyl esters, FAEEs) was preferred to methyl biodiesel (the marketed biofuel) for its better biodegradability, transport and storage properties, and lower emissions of NOx, CO and ultrafine particles (Coniglio et al., 2013, 2014; Navarro-Pineda et al., 2016). Furthermore, fusel oil (a by-product of alcoholic fermentation) could also be used in the ethyl biodiesel and biolubricant production process (Cerón et al., 2018).

Such an alternative would meet the requirement of the global biolubricants market, which is expected to grow much faster than conventional petroleum-based lubricants over the next few years (compound annual growth rate (CAGR) of 5.8% forecast for the 2022–2030 period) (Pawar et al., 2022; Sarker et al., 2023). This trend towards biolubricants is mainly driven by their renewable nature, high biodegradability and low toxicity, as well as improved performance (increased adhesion and lubricity; reduced friction losses in engines and machines that lower energy consumption and, consequently, reduce emissions of harmful gases) (Syahir et al., 2017; Chan et al., 2018; Hossain et al., 2018).

Although the conversion route developed for Indian mustard is very satisfactory (Fig. 1a; Chen et al., 2019; Rapp et al., 2020, 2021), this work proposes to test double transesterification in heterogeneous catalysis to optimize the biolubricant purification step, in particular by avoiding bubble washing. Although most heterogeneous catalysts are more expensive and have a slower reaction rate than homogeneous catalysts, the former can be recovered and reused for other reaction cycles, making the separation process more efficient, cost-effective and environmentally friendly (Boz et al., 2013; Bashir et al., 2022).

In the literature, a range of heterogeneous basic catalysts have been studied for the production of biodiesel (Silveira Junior et al., 2019; Lanfredi et al., 2020; Pedro et al., 2020; Turkkul et al., 2020) and biolubricants (Panchal et al., 2017; Sun et al., 2017; Hossain et al., 2018; Zheng et al., 2018). Among these, potassium carbonate (K_2CO_3) in either supported or unsupported form, was considered attractive due to its very

good performance, low cost, and eco-friendly features (Zheng et al., 2018; Silveira Junior et al., 2019; Pedro et al., 2020). In general, K_2CO_3 is used with catalyst supports (alkaline earth oxide, alumina, hydrotalcite, or bentonite) for biodiesel production, as the catalyst can be partially dissolved in short-chain alcohols such as methanol (Boz et al., 2013). However, K_2CO_3 shows a very low solubility in ethanol at ambient temperature (Pabsch et al., 2022; Schick et al., 2023) and is generally immiscible in longer aliphatic chain alcohols (Zheng et al., 2018), with nonetheless a solubility increasing with the number of hydroxyl functional groups in the alcohol (Naser et al., 2013; Sun et al., 2017; de Caro et al., 2019). This suggests that K_2CO_3 might show partial miscibility with the reaction mixture during IMSO transesterification to produce ethyl biodiesel (further converted into biolubricant by transesterification with 2 EH), but no studies have been found that clearly address this point. For this reason, it was decided in this work to use K_2CO_3 as a catalyst in unsupported form in order to examine its behavior and performance and to analyze potential alternatives that would add further value to the production of the two bioproducts, ethyl biodiesel

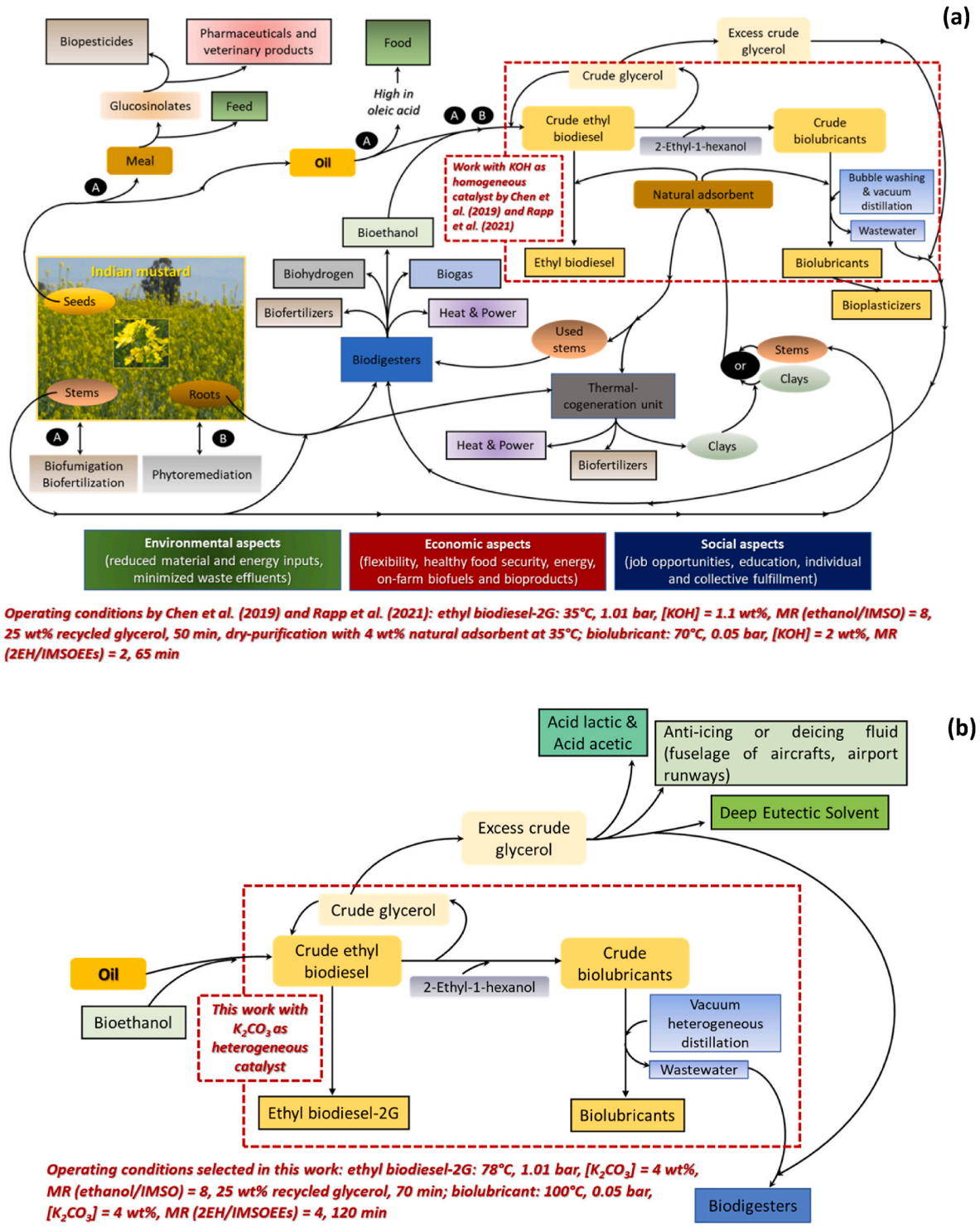

Fig. 1. Main keyword network of the Indian mustard biorefinery. **(a)** Alternative based on KOH homogeneous catalyzed transesterification reactions as proposed by Chen et al. (2019) and Rapp et al. (2021); **(b)** Alternative based on K_2CO_3 heterogeneous catalyzed transesterification reactions as proposed in the present work.

and biolubricant (Fig. 1b). These aspects have never been dealt with in the literature and constitute the novelty brought by this work. In addition, the performance of IMSO in the production of the two bioproducts meeting the standards was compared with that of a synthetic oleic oil (SOO).

2. Experimental

The catalyzed transesterification reactions carried out in this work for the production of ethyl biodiesel and biolubricant are described in Figs. 2–3.

All experiments and analyses were conducted at least in duplicate (in triplicate when disagreement was found). From each set of duplicates, a mean was then calculated and provided as result (for triplicates or more, results are given is terms of mean ± standard deviation).

2.1. Materials

Reagents (citric acid, ethanol, 2-ethylhexanol, and glycerol), solvent (n-heptane), and the chromatographic standards (methyl heptadecanoate and ethyl oleate), all of analytical grade, were purchased from Merck, Acros Organics or Sigma-Aldrich.

For the lipid feedstock, Indian mustard seed oil (IMSO) was obtained by mechanical crushing of the seeds followed by filtration (Rapp et al., 2020), while a synthetic oleic oil (SOO) was also prepared by blending various commercial oils rich in oleic acid. The latter was also prepared in larger quantities in order to assess the impact of scaling up. Characterization of the oils in terms of fatty acid profiles and key properties with respect to ethanolysis are summarized in Tables 1 and 2, while the analytical techniques selected are detailed in Appendix, Table A1 (Caumette et al., 2010; Pohl et al., 2010; Nitièma-Yefanova et al., 2015, 2016; Chen et al., 2019; Ruiz et al., 2023).

Potassium carbonate (K_2CO_3) was supplied from Honeywell Riedel-de Haën in powder form with a purity of over 98 wt%. This commercial K_2CO_3, which will hereinafter be referred to as "Crude", was sieved to obtain three particle size classes: the "Large" ranging from 125 to 325 μm, the "Medium" ranging from 80 to 125 μm, and the "Fine" with particle sizes below 80 μm which turned out to be the most predominant. All K_2CO_3 samples, "Crude", "Large", Medium", and "Fine" were dried (at 110 °C for 3 h), then stored in well-closed glass bottles before using as catalyst in the transesterification reactions. Details of K_2CO_3 catalyst characterization are given in Table 3.

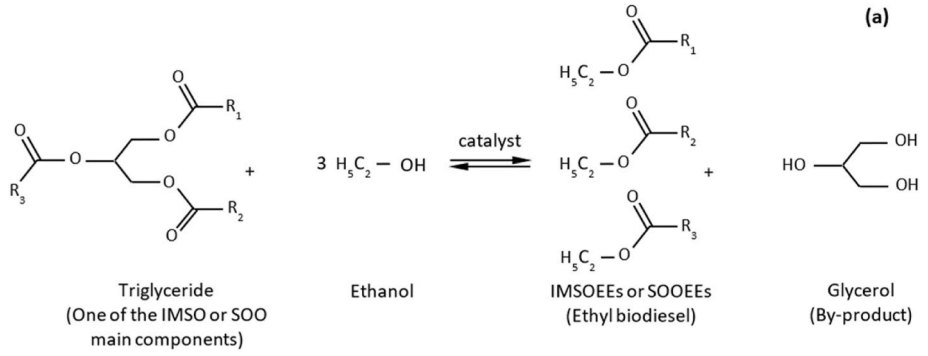

Fig. 2. Catalyzed transesterification reaction of triglycerides involved in IMSO or SOO conversion to ethyl biodiesel. **(a)** Overall chemical equation of triglyceride ethanolysis yielding IMSOEEs or SOOEEs and glycerol; **(b)** Ethanolysis of triglycerides as a sequence of three consecutive and reversible reactions, where $IMSOEE_k$ and $SOOEE_{k,\text{with } k=1 \text{ to } 3}$ are identical or most likely different.

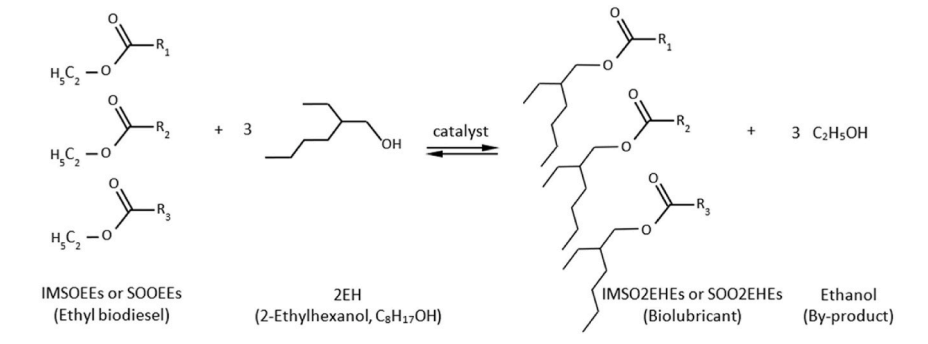

Fig. 3. Catalyzed transesterification reaction of IMSOEEs or SOOEEs (ethyl biodiesel) with 2-ethylhexanol (2 EH) yielding IMSO2EHEs or SOO2EHEs (biolubricant).

Table 1
Fatty acid composition (mass fractions %) of the IMSO and SOO samples used in this work. Major components are indicated in bold. [a]

Fatty acids - Formulae *(name)* [b]	IMSO	SOO
C16:0 *(Palmitic acid)*	3.7 ± 0.1	4.1 ± 0.1
C18:0 *(Stearic acid)*	2.2 ± 0.1	2.8 ± 0.1
C18:1c9 *(Oleic acid)* + C18:1c11 *(cis-Vaccenic acid)*	**38.1 ± 0.3**	**83.4 ± 0.2**
C18:2c9c12 *(Linoleic acid)*	**27.5 ± 0.2**	7.8 ± 0.2
C18:3c9c12c15 *(Linolenic acid)*	**14.4 ± 0.1**	0.1 ± 0.1
C20:1c9 *(Gadoleic acid)*	5.4 ± 0.1	0.6 ± 0.1
C22:1c13 *(Erucic acid)*	6.2 ± 0.1	0.5 ± 0.1
C24:0 *(Lignoceric acid)*	0.3 ± 0.1	0.3 ± 0.1
Total	97.8	99.6
Saturated species	6.2 ± 0.2	7.2 ± 0.1
Monounsaturated species	49.7 ± 0.2	84.5 ± 0.1
Polyunsaturated species	41.9 ± 0.1	7.9 ± 0.1
Average molecular weight as FFAs	279.0	280.4
Average molecular weight as FAEEs (2 EH esters)	307.0 (391.0)	308.4 (392.4)

[a] Fatty acid profiles were determined by methanolysis according to the ASTM D1983 standard for a complete conversion of the glycerides of the oil samples used (IMSO and SOO) into fatty acid methyl esters (FAMEs) which were further quantified by gas chromatography (GC); the standard deviations report the cumulative errors made during methanolysis and quantification. GC equipment and the selected operating conditions are described in Appendix, Table A1.

[b] As example, C18:1c9 means an 18-carbon fatty acid chain with one *cis* double bond (c) located at carbon 9 (starting from the carboxylic group).

Table 2
Key properties of the IMSO and SOO samples used as feedstocks in this work.

Key properties	IMSO	SOO
Average molecular weight [a]	875.0	879.2
Water content (mg/kg) [b]	520 ± 10	518 ± 10
Acid value (mg KOH/g) [b]	1.60 ± 0.02	0.06 ± 0.02
Density at 20 °C (g/mL) [b]	920 ± 0.01	915 ± 0.01
Viscosity at 40 °C (mm^2/s) [b]	32.4 ± 0.1	41.3 ± 0.1
Sulfur content (mg/kg) [b]	21.4 ± 0.2	< LOQ (0.2)
Content in other chemical elements (mg/kg) [b]	< LOQ (0.2–10)	< LOQ (0.2–10)

[a] Calculated from the oil molar composition in terms of fatty acids.

[b] Please, refer to Appendix, Table A1 for details regarding the methods leading to the above given property values (e.g. EN-ISO-12937 for water content, EN-14104 for acid value, EN-ISO-12185 for density, EN-ISO-3104 for viscosity). Particularly, other chemical elements (alkaline, alkaline earth, and metals) have not been detected by ICP-AES or ICP-MS: Ag, Al, As, B, Ba, Ca, Cd, Co, Cr, Cu, Fe, Hg, K, Li, Mg, Mn, Mo, Na, Ni, P, Pb, Sb, Sr, Ti, V, Zn, Zr.

2.2. From the lipid feedstock to ethyl biodiesel via the first transesterification reaction

The water content and acid value of the departure lipid feedstocks IMSO and SOO (Table 2) confirmed that the alkali catalysis was a suitable route to produce the Indian mustard seed oil ethyl esters (IMSOEEs) and the synthetic oleic oil ethyl esters (SOOEEs), respectively. Furthermore, it is worth noting that the sulfur content observed in IMSO (Table 2) is very likely due to the occurrence of glucosinolates, thus limiting the pool of triglycerides that can be converted, as observed in previous studies using Indian mustard oils (Chen et al., 2019; Rapp et al., 2020, 2021).

2.2.1. Conversion procedure for lipid feedstocks

All ethanolysis experiments with IMSO were carried out at atmospheric pressure in a 250 mL three-neck round bottom reactor-flask equipped with a thermometer (±0.5 °C), a reflux condenser, a sampling outlet, and a temperature-controlled magnetic stirrer system (±1 °C) with a PTFE magnetic stir bar. After weighing in the dried reactor-flask, the desired amounts of IMSO and ethanol, the system was heated under constant stirring to the set temperature. Once this temperature was reached, the desired amount of K_2CO_3 catalyst was added, thus defining time zero for the reaction. This procedure was slightly modified for one experiment to assess the impact of heating and the order in which the reactants and catalyst were added on IMSO conversion; in this case, once the mixture of ethanol and K_2CO_3 was prepared in the reactor-flask and had reached the set temperature, IMSO heated separately to the same temperature was subsequently added (thus defining time zero for the reaction).

Table 3
K_2CO_3 catalyst characterization.

(a) Analysis equipment selected and related operating conditions

Objective	Experimental technique	Equipment	Operating conditions
Average particle size (Sauter mean diameter) D [3,2]	Laser diffraction	Malvern Master sizer 2000 (UK)	Size range: 0.02–2000 μm
Surface area and porosity	N_2 (77 K) adsorption/ desorption isotherms + BET (Brunauer-Emmett-Teller) method	Micromeritics Tristar II Plus (USA)	Rapp et al. (2021)

(b) Physical properties

Physical characteristic	K_2CO_3 particle size [b]			
	Fine	Medium	Large	Crude
Average particle size D [3,2] (μm) [a]	27.0	39.6	119	32.5
Smallest particle diameter (μm) [a]	1.45	1.88	4.58	1.65
Specific surface area (m^2/g) [b]	0.1692	0.1536	0.0825	0.1686
Pore volume (cm^3/g) [b]	0.0036	0.0032	0.0017	0.0035
Mean pore width (Å) [b]	58.138	57.852	57.313	58.247

[a] As mentioned in section 2.1, the commercial K_2CO_3 from Honeywell Riedel-de Haën, referred to as "Crude" was sieved to obtain three particle size classes: the "Large" ranging from 125 to 325 μm, the "Medium" ranging from 80 to 125 μm, and the "Fine" with particle sizes below 80 μm.

[a, b] Please refer to part **(a)** of this Table for equipment details and related operating conditions.

By contrast, following the procedure adopted for most IMSO experiments, SOO ethanolysis was carried out in a 1 L glass jacketed reactor, equipped with a PT100 PTFE probe for temperature control (±0.2 °C) and impeller blades mounted via a central drive shaft on an IKA-Eurostar Power Control-Visc stirrer (50–1200 rpm). A four-necked lid allowed completion of the reactor with a condenser and a sampling syringe connected to a long needle. A dead-volume-free valve at the bottom of the reactor allowed the content to be drawn off.

Off-line monitoring of IMSO ethanolysis was conducted by gas-chromatography coupled with a flame ionization detector (GC-FID), at a given sampling frequency (every 2 min for the first 20 min, then every 5 min until 30 min and every 10 min until the end of the experiment). In contrast, SOO ethanolysis was monitored by GC-FID only at the end of experiment. Preliminary identification of the IMSOEEs and SOOEEs was conducted using GC-mass spectrometry (MS). Information specific to the GC-equipment and analysis of samples with preliminary neutralization are given in Appendix, Table A1 (Nitièma-Yefanova et al., 2015, 2016; Muhammad et al., 2017; Chen et al., 2019; Roze et al., 2021).

At the end of the reaction time (60 or 100 min, depending on experiment), a known amount of glycerol was added to the ethanolysis products, previously cooled to 35 °C, to limit the glycerol miscibility in the ester-rich phase. Prior to the addition of glycerol, a three-phase reaction mixture was obtained: the upper phase contained excess ethanol, the intermediate phase was a pseudo-homogeneous mixture of fatty acid ethyl esters (FAEEs) and glycerol, and the lower phase contained the solid catalyst. The addition of glycerol resulted in a two-phase reaction mixture where the biodiesel-rich phase and the glycerol-rich phase can easily be separated by decantation in a separating funnel; note that the glycerol-rich phase contains both the added glycerol and K_2CO_3, in addition to the co-produced glycerol. After removal of the solid catalyst

potentially remaining in the biodiesel-rich phase (vacuum filtration on Sartorius^{TM} nitrate membrane filter 0.2 μm pore size) and evaporation of the remaining ethanol (40 °C, 50 mbar, for 30 min), the resulting product was stored in a tightly sealed flask for characterization and evaluation of its properties as a fuel.

2.2.2. Design of experiments for lipid feedstock conversion

As summarized in Table 4, the ethanolysis experiments were carried out at various operating conditions by modifying successively, the addition order during heating of the reagents to form the reacting mixture, the K_2CO_3 catalyst particle size, the ethanol to oil molar ratio (MR), the reaction temperature, and the glycerol addition protocol (at various percentage: 0, 15, or 25 wt%, and with or without cooling the reaction mixture to 35 °C first). In contrast, the amount of lipid feedstock, the stirring speed and the mass concentration of catalyst were held constant for all experiments (50 g and 250 rpm for IMSO, 300 g and 700 rpm for SOO, with $[K_2CO_3] = 4$ wt% based on the initial mass of oil). All values were selected based on previous studies **(**Silveira Junior et al., 2019; Lanfredi et al., 2020; Rapp et al., 2021**)** and then optimized to obtain the conversion of the lipid raw materials used in this work, while considering the environmental and energy impacts of the conversion process.

2.3. From ethyl biodiesel to biolubricant via the second transesterification reaction

The fractions of IMSOEEs and SOOEEs that were not dedicated to characterization and biofuel property estimation (section 2.4) were converted by K_2CO_3 alkaline transesterification with 2-ethylhexanol (2 EH) to obtain the targeted biolubricant, that is IMSO2EHEs and SOO2EHEs, respectively. Since the same catalyst was used for the second transesterification step, the removal of K_2CO_3 by filtration (section 2.2) was not essential, other than quantifying the amount of catalyst introduced in the reaction mixture and the characteristics of the IMSOEEs and SOO2EHEs used as starting reactants (molecular species composition, including K content, as shown in Table 6 in the "Results and discussion" section).

2.3.1. Conversion procedure for ethyl biodiesels

The biolubricant production was performed in a laboratory scale batch reactive distillation unit operating under low pressure. This option helped reduce the reaction temperature (2 EH normal boiling point: 184.6 °C) and reaction time, minimizing energy costs, facilitating by-product (ethanol) removal from the reaction mixture and increasing biolubricant yield (by shifting the transesterification chemical equilibrium in favor of product formation) **(**Chen et al., 2019; Rapp et al., 2021; Coniglio et al., 2013**)**. The transesterification reaction of ethyl biodiesels to biolubricants was conducted in a 500 mL four-neck round bottom reactor-flask equipped with a thermometer (±0.5 °C), a sampling outlet, and a temperature-controlled magnetic stirrer system (±1 °C) with a PTFE magnetic stir bar. A Vigreux column topped by a second thermometer (±0.5 °C) was attached at one end to the reactor-flask and at the other to a Liebig condenser connected to a vacuum take-off adapter for attachment, via a three-way valve, to the vacuum pump and the flasks for collecting the distillate (ethanol). The Liebig condenser was cooled with a recirculating silicon oil bath (0 °C) and the two collection flasks with an ice bath. After weighing the desired amounts of biodiesel (IMSOEEs or SOOEEs) and 2 EH in the previously dried reactor-flask, the system was heated under constant stirring to the selected temperature. Once this temperature was reached, the desired amount of K_2CO_3 catalyst was added and the three-way valve was switched to connect the reactive distillation unit to the vacuum pump, thus defining time zero for the reaction.

Off-line monitoring of biodiesel transesterification was conducted by GC-FID at a given sampling frequency (30-min intervals until the end of experiment set to 120 min). As with IMSOEEs and SOOEEs, the preliminary identification of IMSO2EHEs and SOO2EHEs was carried out by GC-MS, and information specific to GC-equipment and sample analysis is given in Appendix, Table A1 (Nitièma-Yefanova et al., 2015, 2016; Muhammad et al., 2017**;** Chen et al., 2019; Roze et al., 2021**)**.

Afterwards, the biolubricants (IMSO2EHEs and SOO2EHEs) were purified by removing first the solid catalyst by vacuum filtration (on Sartorius^{TM} nitrate membrane filter 0.2 μm pore size) and then most of the excess 2 EH by vacuum fractional distillation (0.03 bar, 110 °C); the remaining 2 EH was eliminated by vacuum heterogenous distillation after addition of water (0.01 bar, 43 °C).

2.3.2. Design of experiments for ethyl biodiesel conversion

As summarized in Table 5, the biodiesel conversion experiments were carried out at various operating conditions by successively modifying the reaction temperature, the MR of 2 EH to biodiesel (IMSOEEs or

Table 5
Operating conditions of the most relevant experiments of biolubricant production via ethyl biodiesel conversion. Each operation variable was changed sequentially by remaining constant the other variables. Optimal operating conditions are indicated in bold. [a]

Experiment	Feedstock (relating biodiesel synthesis expt. [b])	T (°C)	2 EH to biodiesel MR	$[K_2CO_3]$ (wt %) [c]
ExpB1	SOOEEs (ExpA2)	95	3:1	3
ExpB2	SOOEEs (ExpA2)	95	4:1	3
ExpB3	SOOEEs (ExpA2)	100	4:1	3
ExpB4	**SOOEEs (ExpA2)**	**100**	**4:1**	**4**
ExpB5	SOOEEs (ExpA2)	100	4:1	5
ExpB6	IMSOEEs (ExpA1)	100	4:1	5
ExpB7	IMSOEEs (ExpA6)	100	5:1	5
ExpB8	**IMSOEEs (ExpA7)**	**100**	**4:1**	**4**

[a] The amount of biodiesel, stirring speed and reaction pressure remained unchanged for all experiments (40 g, 250 rpm and 0.05 bar).
[b] Please, refer to Table 4 for the referred experiment.
[c] "Crude" K_2CO_3 on basis of the initial oil mass.

Table 4
Operating conditions of the most relevant ethanolysis experiments. Each operating variable has been modified sequentially by remaining constant the other variables. Optimal operating conditions are indicated in bold. [a]

Experiment	Feedstock	Temperature (°C)	Ethanol to oil MR	Ethanol and oil heating	K_2CO_3 sample in terms of particle size [b]	Glycerol addition [c] (temperature)
ExpA1	IMSO	70	15:1	separately	"Crude"	25 wt% (35 °C)
ExpA2	IMSO; SOO	70	15:1	together	"Crude"	25 wt% (35 °C)
ExpA3	IMSO	70	15:1	together	"Medium"	None (−)
ExpA4	IMSO	70	15:1	together	"Large"	15 wt% (35 °C)
ExpA5	IMSO	70	15:1	together	"Fine"	15 wt% (70 °C)
ExpA6	IMSO	70	8:1	together	"Crude"	15 wt% (35 °C)
ExpA7	IMSO	**78**	**8:1**	**together**	**"Crude"**	**25 wt% (35°C)**

[a] For all experiments: P = 1.01 bar, stirring speed set to 250 rpm, $[K_2CO_3] = 4$ wt% on basis of the initial oil mass, and lipid feedstock: IMSO, with the exception of ExpA2 that was also conducted with SOO to produce SOOEEs as biodiesel, for comparison with a different oleic oil and a larger scale (× 6, see section 2.2).
[b] "Crude": commercial K_2CO_3 sample without sieving treatment; "Fine", "Medium", and "Large": samples of commercial K_2CO_3 after sieving leading respectively to particle size inferior to 80 μm, or ranging from 80 to 125 μm, or from 125 to 315 μm.
[c] On basis of the initial oil mass.

Table 6
Some functional physico-chemical properties and ester composition of the biofuels and biolubricants produced in this work [a].

(a) Functional physico-chemical properties

Property	IMSOEEs	SOOEEs	Biodiesel specifications EN-14214 [min; max]	IMSO2EHEs	SOO2EHEs	Biolub of reference Valtris Enterprises Francee (2023) [b]	Standard deviations [c]
Acid value (mg KOH/g)	0.12	0.03	[-; 0.50]	0.18	0.34	0.50	±0.02
Water content (mg/kg)	589	741	[-; 500]	512	619	510	20
Fatty acid esters (wt%)	97.20	98.15	[-; 96.5]	95.68	96.63	–	0.08
Monoglycerides (wt%)	2.05	0.70	[-; 0.80]	–	–	–	0.05
Diglycerides (wt%)	0.30	0.14	[-; 0.20]	–	–	–	0.05
Triglycerides (wt%)	0.04	0.00	[-; 0.20]	–	–	–	0.05
Free glycerol (wt%)	0.05	0.02	[-; 0.02]	–	–	–	0.003
Total glycerol (wt%)	0.62	0.22	[-; 0.25]	–	–	–	0.05
Alkali metals Na + K (mg/kg) [d]	< LOQ (10)	< LOQ (10)	5	< LOQ (10)	< LOQ (10)	–	±0.01
Color (Gardner)	–	–	[-; -]	4.2	0.6	1.0	±0.2
Color (Hazen)	–	–	[-; -]	801	119	100	±2
Density (kg/m^3) at 20 °C	878	871	[860; 900]	873	869	870	$\pm 3{\cdot}10^{-5}$
Viscosity (mm^2/s) at 40 °C	4.8	4.9	[3.5; 5.0]	8.1	8.7	9.0	±0.1
Flash point (°C)	428	423	[101; -]	–	–	–	±12
Cloud point (°C)	−4.6	−6.2	[-12; −3]	–	–	–	±1
Pour point (°C)	−8.3	−10.6	[-16; −5]	–	–	−69	±2
Cold filter plugging point (°C)	−10.5	−12.4	[-; -]	–	–	–	±0.1
Higher heating value (MJ/kg)	41.36	41.43	[-; -]	–	–	–	±0.1
Oxidation stability at 110 °C (hrs)	6.46	7.62	[6; -]	–	–	–	±0.1

(b)Percent mass composition of the identified esters (IMSOEEs for the biofuel samples; IMSO2EHEs for the biolubricant samples)

Liquid bioproduct	C16:0	C18:0	C18:1 (oleate & cis-vaccenate)	C18:2	C18:3	C20:1	C22:1	C24:0
IMSOEEs	3.48	2.21	37.62	27.80	14.98	4.80	6.07	0.23
SOEEs	3.87	2.69	83.27	7.89	0.06	0.24	0.10	0.03
IMSO2EHEs [e]	3.63 (0.15)	2.28 (0.10)	37.98 (1.72)	27.56 (1.25)	14.15 (0.64)	4.40 (0.20)	5.66 (0.28)	0.02 (0.00)
SOO2EHEs [e]	3.99 (0.13)	2.69 (0.08)	81.42 (2.85)	7.92 (0.28)	0.00 (0.00)	0.61 (0.02)	0.00 (0.00)	0.00 (0.00)

[a] Please, refer to Appendix, Table A1 for details regarding the methods leading to the given property values.
[b] This biolubricant was produced with the same alcohol as the one selected in this work (2 EH) but with rapeseed oil as lipid feedstock.
[c] These standard deviations are common to the determination of both biofuel and biolubricant specific functional physico-chemical properties conducted in this work.
[d] Other chemical elements (alkaline, alkaline earth, and metals) have not been detected by ICP-AES or ICP-MS: Ag, Al, As, B, Ba, Ca, Cd, Co, Cr, Cu, Fe, Hg, K, Li, Mg, Mn, Mo, Na, Ni, P, Pb, Sb, Sr, Ti, V, Zn, Zr.
[e] Are given in brackets the percent mass fractions of the remaining IMSOEEs.

SOOEEs), and the catalyst mass concentration. In contrast, the amount of biodiesel, stirring speed, and reaction pressure remained unchanged for all experiments (40 g, 250 rpm and 0.05 bar, respectively) using the catalyst whose particle size gave the best biodiesel production results (i.e. "crude" K_2CO_3). All these values were selected based on previous findings (Sun et al., 2017; Zheng et al., 2018; Rapp et al., 2021) and then optimized to obtain the best conversion of ethyl biodiesel while considering environmental and energy impacts.

2.4. Bioproduct characterization and evaluation of the biofuel and biolubricant properties

Characterization of liquid bioproducts was carried out by assessing key molecular species such as triacylglycerides (TGs), diacylglycerides (DGs), monoacylglycerides (MGs), free glycerin, esters (IMSOEEs, SOOEEs, IMSO2EHEs, and SOO2EHEs), and alcohols (ethanol and 2 EH), all ascertained by GC-FID; in contrast, water content was determined by Karl Fischer titration. In addition, potassium and heavy metals (resulting respectively from the potential leaching of the selected catalyst K_2CO_3 and possibly from the extraction step of IMSO and oleic oils blended to obtain the SOO used in this work) were also quantified using inductively coupled plasma-atomic emission spectroscopy (ICP-AES) and inductively coupled plasma-mass spectrometry (ICP-MS).

Some functional properties of the final biofuel and biolubricant (acid value, color, density, viscosity, flash point, cloud point, pour point, and cold filter plugging point) were evaluated too, in accordance with ASTM and ISO standards or theoretical estimation methods.

The equipment and operating conditions or estimation methods selected to collect this information are described in Appendix, Table A1 (Caumette et al., 2010; Pohl et al., 2010; Carareto et al., 2012; Hong et al., 2014; Bolonio et al., 2015; Nitièma-Yefanova et al., 2015, 2016; Muhammad et al., 2017; Chen et al., 2019; Roze et al., 2021; Ruiz et al., 2023; Valtris Enterprises France, 2023).

3. Results and discussion

The key species content of the reaction mixture as a function of time for each of the transesterification processes leading to ethyl biodiesel or biolubricant are shown in Figs. 4 and 5 respectively, while the functional physico-chemical properties of the two resulting bioproducts are presented in Table 6.

3.1. Ethyl biodiesel production via the first transesterification reaction

For all operating conditions, the FAEE contents increased very slowly at the early stage of the reaction, then rapidly over a short period, finally approaching asymptotically the chemical equilibrium imposed by the initial composition and temperature of the reaction mixture (Fig. 4). These sigmoidal profiles are typical of reactions under control of three successive mechanisms: mass transfer, kinetics, and chemical equilibrium. However, IMSO ethanolysis in homogeneous catalysis proved to be under the control of the latter two mechanisms only, primarily because the high solvent power of ethanol limited mass transfer between the reagents (Nitièma-Yefanova et al., 2015, 2016, 2017; Rapp et al., 2021). Consequently, the behavior observed at the start of ethanolysis in heterogeneous catalysis is mainly due to the limitation of internal mass transfer, i.e. within the catalyst pores, and very little to the limitation of external mass transfer induced by the immiscibility of the reactants, i.e.

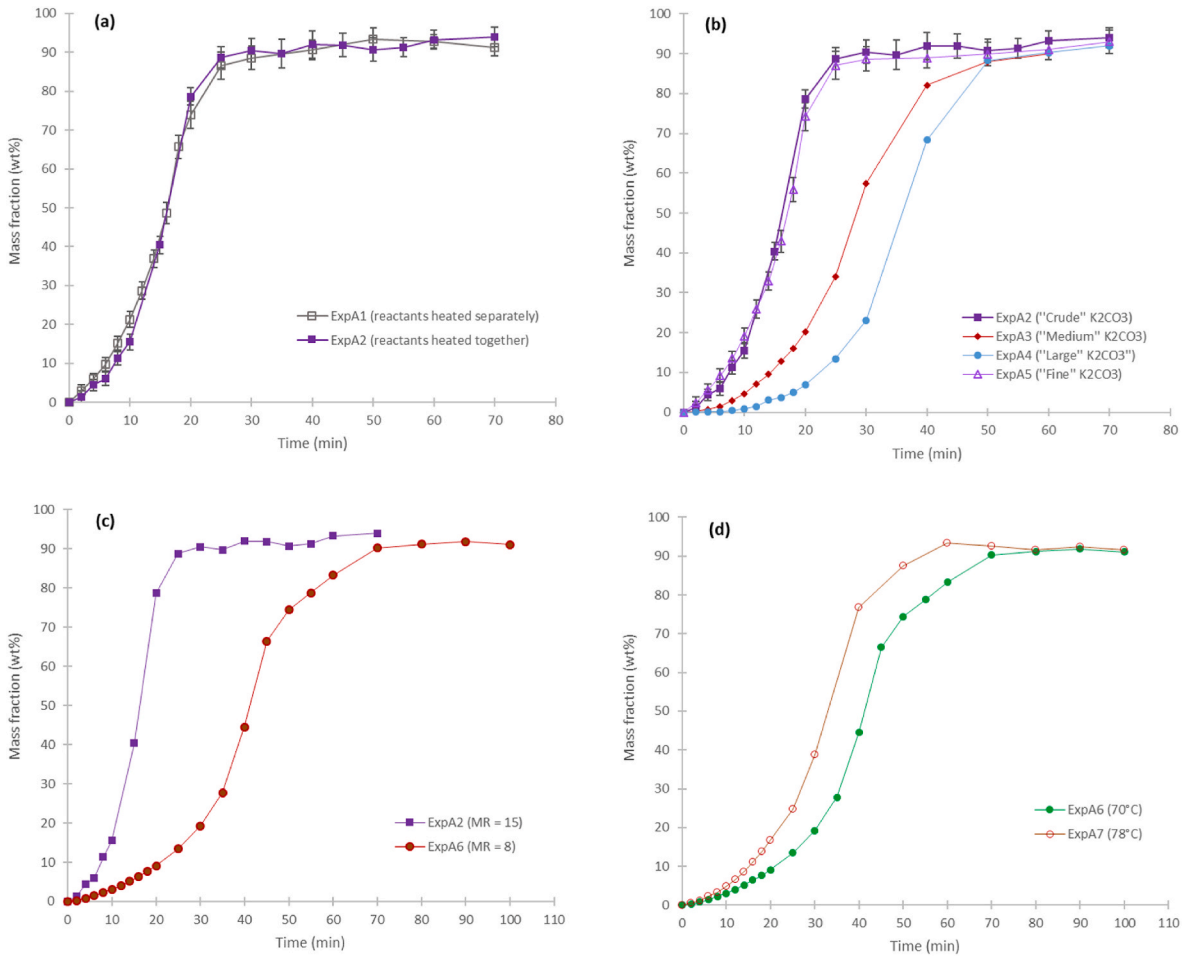

Fig. 4. Mass fractions of IMSOEEs as a function of reaction time for various operating conditions (all detailed in Table 4): **(a)** different heating protocols of the reactants, ethanol and IMSO; **(b)** various K_2CO_3 catalyst particle sizes; **(c)** various ethanol to oil MR; **(d)** different reaction temperatures.

ethanol and IMSO. Besides, it was observed (similarly to Nitièma-Yefanova et al., 2015, 2016, 2017; Rapp et al., 2021, in homogeneously catalyzed NEVO ethanolysis) that the reaction mixture at time zero of the reaction exhibited two liquid phases due to the partial immiscibility of ethanol and triglycerides. However, as soon as a sufficient quantity of FAEEs was formed in the medium, the reaction mixture became less turbid, and then homogenous. Subsequently, when the reaction has progressed sufficiently to lead to the formation of FAEEs and glycerol in such proportions that the two products are no longer totally miscible (under reaction temperature and pressure conditions), the medium became cloudy again and demixed into two liquid phases in the form of a pseudo-homogenous mixture of a glycerol-rich phase dispersed in small droplets in an ester-rich phase, thus marking chemical equilibrium. Therefore, vigorous mixing (increasing the contact area between reagents) was adopted for all experiments, particularly before chemical equilibrium was reached, to cope with mass transfer limitation.

Moreover, in the presence of the heterogeneous K_2CO_3 catalyst, ethanol and glycerides from IMSO (or SOO) probably react according to an Eley-Rideal mechanism where the alcohol adsorbs onto the catalyst surface to form the adsorbed active species ethanolate, which can then react with the second reactant remaining in solution (a tri-, di- or monoglyceride molecule) to produce the target product (diglyceride, monoglyceride or FAEE) and the co-product glycerol.

Furthermore, as the choice was made in this work to use the K_2CO_3 catalyst in unsupported form, it was observed that K_2CO_3 dissolved in the glycerol produced during ethanolysis. This was an expected risk given the increasing solubility of K_2CO_3 with the number of hydroxyl functional groups in the alcohol reported in the literature (Naser et al., 2013; Sun et al., 2017; de Caro et al., 2019). So, while separating K_2CO_3 from glycerol for reuse in new catalysis cycles would make no sense, an interesting option would be to valorize the available [K_2CO_3 + glycerol] mixtures for valuable applications such as green anti-icing or de-icing fluid for aircraft fuselage (Baroi et al., 2009), deep eutectic solvents used to replace ionic liquids (Naser et al., 2013), or catalytic synthesis of the two platform molecules lactic and formic acids, simultaneously (Ainembabazi et al., 2020).

3.1.1. *Heating protocols of the reactants*

Heating the ethanol with K_2CO_3 catalyst first, to form the active species before adding the preheated IMSO, should accelerate the reaction compared with adding the catalyst once the reagents (heated together) reach the desired temperature. As shown in Fig. 4a, there is a slight difference in results between these two protocols (error bars do not overlap the first 10 min of the reaction). Thus, separate heating of the reactants accelerates the reaction at the start (ExpA1, Fig. 4a), confirming the Eley-Rideal mechanism assumed to form the adsorbed active species ethanolate on the catalyst surface. However, the gap between the two experiments rapidly narrows and the conversions obtained become similar once chemical equilibrium is reached. Besides, it is more practical to heat the reagents, ethanol and IMSO (or SOO) together before adding the catalyst, to better control the start of the reaction. Therefore, all subsequent experiments were carried out using this heating protocol (ExpA2, Fig. 4a).

3.1.2. *Catalyst particle size*

As shown in Fig. 4b, the larger the catalyst particles (offering the reaction medium a smaller specific surface area, pore volume and pore

width, Table 3), the slower the reaction. These observations confirm the limitation of internal mass transfer within the catalyst pores at the early stage of the reaction (including the hypothesis of a heterogeneous catalysis process according to the Eley-Rideal mechanism). Nevertheless, whatever the size of the catalyst particles, all experiments eventually achieved similar conversions at equilibrium. Moreover, the smallest catalyst particles gave similar results to the "crude" K_2CO_3 (ExpA5 vs ExpA2, Fig. 4b), which was expected as the "crude" K_2CO_3 used was 95 wt% "fine" K_2CO_3 with particle size of less than 80 μm (Table 3). Consequently, the "crude" K_2CO_3 corresponding to the commercial chemical with the characteristics of a mesoporous material known to have a better catalytic efficiency (Sun et al., 2017) was retained thereafter (average pore width of 20–500 Å).

3.1.3. Ethanol to oil molar ratio

The ethanol to oil MR has a significant impact on both the reaction yield and the production cost (Silveira Junior et al., 2019). Theoretically, the stoichiometry of the overall reaction is 1 mol of triglyceride for 3 mol of ethanol; however, because transesterification is a reversible reaction (Fig. 2), the chemical equilibrium had to be shifted toward FAEE formation by operating with excess ethanol and withdrawing the byproduct glycerol from the reactive medium (Zheng et al., 2018; Coniglio et al., 2014). As shown in Fig. 4c, increasing the ethanol to oil MR (from 8 to 15, ExpA6 vs ExpA2) significantly accelerated the reaction rate (by increasing the number of adsorbed active species ethanolate due to a larger amount of reagent). Nonetheless, this MR increase did not significantly affect the plateau reached at chemical equilibrium (very likely because the adopted MR are larger than the critical value of 6 as mentioned by Nitièma-Yefanova et al., 2016), so that the same conversion was achieved at the end of transesterification. The use of a high MR leads to additional investment costs and operational difficulties during the separation process (Encinar et al., 2021). However, a longer

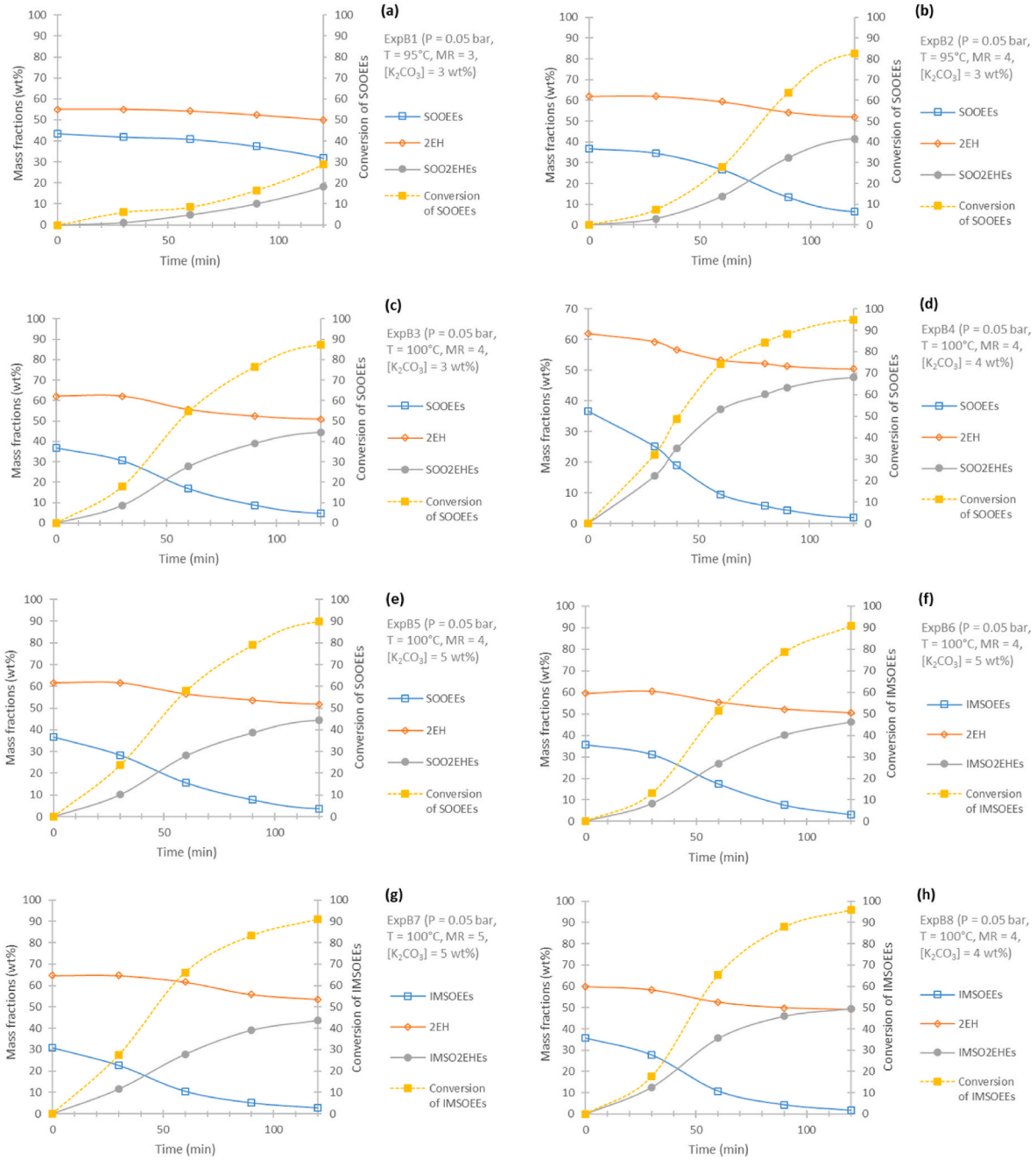

Fig. 5. Species mass fractions and conversion as a function of reaction time during transesterification of crude ethyl biodiesel (IMSOEEs or SOOEEs) to biolubricant (IMSO2EHEs or SOO2EHEs, respectively) at the operating conditions of the most relevant experiments carried out in this work (details in Table 5).

reaction time (induced by a lower MR) implies higher operational costs (due to additional heating over a longer period). A techno-economic analysis would therefore be useful to make an appropriate decision on the MR value, unless the reaction can be significantly accelerated by a slight increase in temperature.

3.1.4. Temperature of reaction

The effect of temperature on IMSO transesterification was studied at 35 °C, 70 °C, and 78 °C (with ethanol/oil MR = 8 and [K_2CO_3] = 4% by weight, Fig. 4d). As expected from Arrhenius' law, temperature had a positive impact on reaction kinetics. Nonetheless, at 35 °C no ester was detected by GC-FID, leading to the conclusion that the reaction did not take place. A higher reaction temperature was required to form the adsorbed ethanolate active species (while additionally helping overcome the internal and external mass transfer limitations). Although the reaction rate is clearly faster at 78 °C than at 70 °C (ExpA7 vs ExpA6, Fig. 4d), the temperature difference (8 °C) between these two experiments appears to be too small to have a significant influence on the chemical equilibrium (similar FAEE mass fractions are obtained at the end of these experiments). Combined with a high ethanol to oil MR, this result is consistent with previous work where the exothermicity of the ethanolysis reaction was observed with a more pronounced effect on the amount of product formed the lower the ethanol to oil MR (Nitièma-Yefanova et al., 2016; Chen et al., 2019). Since it should be more cost-effective to heat the reaction mixture 8 °C more with a smaller MR, transesterification of IMSO at 78 °C with MR = 8 was retained.

3.1.5. Glycerol addition

Due to the high solvent power of ethanol leading to the formation of a pseudo-homogenous mixture at chemical equilibrium of the reaction, glycerol was added at the end of ethanolysis to induce a clear liquid-liquid demixing (Table 4). It is important that this procedure be conducted at ambient temperature to be effective (35 °C max.) because of the increase of glycerol miscibility in the ester-rich phase with temperature (addition of glycerol without cooling the reaction mixture resulted in a decrease in FAEE content of approx. 5 wt%). The best results were observed at 25 wt% glycerol (based on the initial weight of oil) which was similar to previous work by Nitièma-Yefanova et al. (2016) and Chen et al. (2019) on homogeneous catalytic ethanolysis of various NEVOs (the addition of 0–15 wt% glycerol proved insufficient in this work to induce clear demixing).

3.1.6. Scaling up and different lipid feedstock

Ethanolysis of SOO gave SOOEEs contents similar to that achieved with IMSO under the same operating conditions (ExpA2, Table 4 and Fig. 4); this result obtained on a larger scale (× 6) suggests a satisfactory transfer to pilot scale, at least for similar NEVOs.

3.2. Biolubricant production via the second transesterification reaction

The transesterification being a reversible reaction (Fig. 3), the chemical equilibrium was shifted toward biolubricant formation by operating with excess 2 EH and withdrawing the byproduct ethanol from the reactive medium via vacuum distillation.

The mass fraction profiles vs time of the biolubricants (IMSO2EHEs and SOO2EHEs) produced by transesterification of the ethyl biodiesels (IMSOEEs and SOOEEs) with 2 EH are presented in Fig. 5 for the most significant experiments carried out in this work. Unfortunately, the cooling system of the vacuum reactive distillation unit was not efficient enough to trap all ethanol released during transesterification. Consequently, the mass fraction profiles vs time are depicted for all reaction mixture species except ethanol. The key points highlighted by all the experiments are discussed below.

As shown in Fig. 5, the mass fractions vs time profiles of the species in the reaction mixture are very similar to the profiles obtained from IMSO ethanolysis (Fig. 4). As expected, the curves show the specific characteristics of any reversible reaction under internal diffusional control (mass transfer limited only within the catalyst pores, the reactants ethyl biodiesels and 2 EH being miscible here), then under kinetic and thermodynamic control, successively.

Raising the temperature (from 95 to 100 °C) had a significant positive impact throughout this second transesterification, successively helping to overcome the internal diffusion regime, then accelerating the reaction via the increase in the rate constant, and finally improving the conversion of biodiesel at the chemical equilibrium (ExpB2 vs ExpB3, Fig. 5b–c). This last point reveals that the transesterification of ethyl biodiesels with 2 EH is an endothermic reaction, as observed by others (Zheng et al., 2018). Although a further increase in temperature could have improved the process, temperatures above the boiling point of 2 EH (103 °C at 0.05 bar) were not examined because the laboratory-scale reactive distillation unit used in this work was not equipped with reflux.

The 2 EH to biodiesel MR also had a significant positive impact on biolubricant production regardless of whether the transesterification reaction was under internal diffusion, kinetic, or thermodynamic control (ExpB1 vs ExpB2, Fig. 5a–b; ExpB6 vs ExpB7, Fig. 5f–g). The effect is much more noticeable when decreasing the MR value from 4 to 3 (i.e. from four to three times the theoretical stoichiometry of the reaction, Fig. 3), the latter value thus appearing to be a limiting value (ExpB2 vs ExpB1, Fig. 5b–a). Nevertheless, increasing the MR from 4 to 5 helped to speed up the reaction initially, but with no significant change when chemical equilibrium was reached (ExpB6 vs ExpB7, Fig. 5f–g).

As expected, increasing the catalyst concentration from 3 to 4 wt% accelerated the reaction without changing the chemical equilibrium (ExpB3 vs ExpB4, Fig. 5c–b). However, a further increase in the catalyst concentration led to poorer results (ExpB4 vs ExpB5, Fig. 5d–e; ExpB8 vs ExpB6, Fig. 5h–f). A similar tendency was also observed in the literature with K_2CO_3 supported on hydrotalcite or γ-alumina as heterogenous catalyst for biodiesel or biolubricant production (Sun et al., 2017; Silveira Junior et al., 2019). In the context of our work, this behavior could be explained by the saturation of the reactive medium with catalyst, leading to a reduction in the number of catalyst pores accessible to the 2 EH reagent, and therefore to a decrease in the number of adsorbed 2 EH active species (assuming an Eley-Rideal type mechanism, similar to ethanolysis).

Moreover, similar results were obtained for the two ethyl biodiesels (SOO2EHEs and IMSO2EHEs) confirming that the process is transposable, at least with similar reagents, both in terms of fatty alcohol and fatty esters (ExpB5 vs ExpB6, Fig. 5e–f; ExpB4 vs ExpB8, Fig. 5d–h).

Thus, reactive distillation under low pressure proved to be a relevant option, allowing shifts in chemical equilibrium towards formation of biolubricant by removal of ethanol from the reacting mixture, thus improving reaction conversion and product purity. Under the optimal pressure of 0.05 bar (other operating conditions: 100 °C, MR = 4, [K_2CO_3] = 4 wt %) more than 95 wt % of the departure FAEEs (SOOEEs or IMSOEEs) were converted in less than 120 min (Fig. 5d and h). However, a higher content in IMSO2EHEs would have been obtained if the departure IMSO had been pre-treated to increase the glyceride pool, and thus the IMSOEE content. Although catalyst reusability was not examined in this work, the literature (Zheng et al., 2018) mentions that K_2CO_3 can be reused up to five times in biolubricant production without observing any loss of activity.

3.3. Bioproduct key properties

Key functional physico-chemical properties and ester composition of the biofuels (IMSOEEs and SOOEEs) and biolubricants (IMSO2EHEs and SOO2EHEs) produced in this work are shown in Table 6.

The selected transesterification procedure was observed to be effective. Indeed, no potassium (K) was detected by ICP-AES/ICP-MS (K content below the LOQ of the analytical method), confirming that K_2CO_3 can actually be considered a heterogeneous catalyst in this work. Furthermore, high ester contents were obtained for both bioproducts, i.e. over 97 wt% for the ethyl biofuels and 95 wt% for the biolubricants

(with production yields of 96% and 93% respectively, from reaction through catalyst filtration to alcohol removal). Higher-purity biodiesels and biolubricants, ranging from 99 wt% to almost 100 wt%, have been obtained in the literature, but by transesterification of different raw materials (palmitic acid methyl ester and 2-ethylhexanol by Zheng et al., 2018; sunflower oil and ethanol by Silveira Junior et al., 2019; rapeseed oil and methanol, then 2-ethyl-2-hydroxymethyl-1,3-propadiol by Encinar et al., 2021). The ester contents obtained in this work should be improved by removing glucosinolates from the IMSO prior to the transesterification reaction and conducting the process on a pilot scale (Nitèma-Yefanova et al., 2017).

Most biofuel specifications of IMSOEEs and SOOEEs were met. The few exceptions were the contents in water for SOOEEs and in MGs and DGs for the IMSOEEs, which should be handled without major inconvenience by dry-purification using a natural adsorbent (the Montmorillonite clay to reduce water content and the Indian mustard stems to reduce MG and DG contents; Rapp et al., 2020, 2021). It should also be mentioned that the sulfur (S) species initially observed by ICP-AES/ICP-MS in IMSO (around 21 mg/kg, Table 2) was no longer detected in IMSOEEs. This reveals that the glucosinolates initially present in IMSO were converted (into molecules other than FAEEs) during ethanolysis. The presence of species other than glycerides (pool convertible to FAEEs) in IMSO may explain the lower content of IMSOEEs than SOOEEs. Nevertheless, the IMSOEE product obtained had very satisfactory physical properties as a biodiesel, as did SOOEEs derived from SOO synthetic oil (Table 6). The IMSOEEs product is therefore a good candidate for further research with thermal and emission analyses, to obtain a significant diagnosis.

Biolubricant quality specifications of IMSO2EHEs and SOO2EHEs were achieved for the basic properties of density, viscosity and color (Table 6) (Habib et al., 2014; McNutt and He, 2016; Zheng et al., 2018). The higher color indicator (Gardner and Hazen) observed for the IMSO2EHEs was caused by the color of the parent oil, i.e. orange for the IMSO but pale-yellow for the SOO and the rapeseed oil used as lipid feedstock for the Biolub of reference (Valtris Enterprises France, 2023). The thermo-oxidative stability and cold-flow properties of the biolubricants produced could not be assessed in this work, so one might be concerned at the high content of polyunsaturated species in the IMSO2EHEs produced (42% by weight) compared with the monounsaturates (48% by weight), containing oleic esters to a large extent (38% by weight) and also longer-chain esters from C20 to C24 (Table 6b). Indeed, a low degree of unsaturation improves thermo-oxidative stability, but a certain number of unsaturation sites is required to obtain adequate cold flow properties (while increasing fatty chain length leads to higher viscosity). For this reason, vegetable oils with a high oleic acid content are considered optimal for producing high-performance biolubricants (Reeves et al., 2015; Chen et al., 2019; Rapp et al., 2021). Nonetheless, addition of citric acid as a natural antioxidant could enhance the oxidation stability of the IMSO2EHEs produced (Sharma and Biresaw, 2016). Furthermore, if viscosity needs to be improved for a specific application, ethyl cellulose (EC), which in small quantities can improve this property by a factor of two, could be used as an additive (Chan et al., 2018). In addition, Indian mustard stems are rich in cellulose (Rapp, 2018) and could therefore be used to produce EC, further expanding the contours of a biorefinery system based on Indian mustard. As a result, all these considerations suggest that the obtained IMSO2EHE product is a potential candidate as biolubricant, particularly as a metalworking fluid.

4. Conclusions

The two transesterification routes studied in this work, converting IMSO into an energy carrier (IMSOEEs) and then into a biolubricant (IMSO2EHEs), gave positive results, similar to those obtained with synthetic oleic oil (SOO) prepared by blending various commercial oils rich in oleic acid. ICP-AES/ICP-MS analyses of both bioproducts confirmed that K_2CO_3 played a role as a heterogeneous catalyst. Although K_2CO_3 cannot be recycled and reused for further biodiesel production cycles because of its solubility in glycerol, the [glycerol + K_2CO_3] mixtures generated through this transesterification route can have various major applications (as anti-icing or de-icing fluid for aircraft fuselage, deep eutectic solvents, or even reacting mixture for simultaneous synthesis of lactic and formic acids as illustrated in Fig. 1b; Baroi et al., 2009; Naser et al., 2013; Ainembabazi et al., 2020).

Regarding the production of the ethyl biodiesels (IMSOEEs and SOOEEs) by ethanolysis of the lipid feedstocks (IMSO and SOO), optimized operating conditions (78 °C, 1.01 bar, 4 wt% K_2CO_3, ethanol to oil molar ratio of 8, 60 min, and addition of glycerol at 35 °C at the end of the reaction) resulted in biofuels with high purity (over 97 wt%) and key functional physicochemical properties (acid value, density, viscosity, flash point, cloud point, pour point, cold filter plugging point, higher heating value, and oxidation stability) in compliance with EN 14214 standards. Nevertheless, a higher content in IMSOEEs might be obtained with a pre-treatment of the IMSO to remove species that are not glycerides, such as glucosinolates.

Regarding the production of the biolubricants (IMSO2EHEs and SOO2EHEs) by transesterification of ethyl biodiesels (IMSOEEs and SOOEEs) with 2 EH, the choice of reactive distillation with optimized operating conditions (100 °C, 0.05 bar, 4 wt% K_2CO_3, 2 EH to IMSOEEs molar ratio of 4, and 120 min) yielded biolubricants with high purities (around 96 wt%) and key functional physicochemical properties (density, viscosity, and color) that met the requirements of metalworking fluids.

Given the mild operating conditions and the performance for various NEVOs of ethanolysis by homogeneous catalysis, it would be interesting to explore a hybrid alternative with a first step of ethyl biodiesel production by homogeneous catalysis as performed in previous works (Nitièma-Yefanova et al., 2015, 2016, 2017; Chen et al., 2019; Rapp et al., 2021) and a second step of biolubricant production by heterogeneous catalysis as performed in this work. Moreover, this hybrid alternative will have to be conducted at a pilot scale to account for costs and environmental considerations more realistically than at a laboratory scale.

CRediT authorship contribution statement

Déya Regragui: Investigation, Data curation. **Dg Arina Amira Binti Matlan:** Investigation, Formal analysis, Data curation. **Graeme Rapp:** Writing – review & editing, Resources. **Richard Trethowan:** Writing – review & editing, Resources. **Alejandro Montoya:** Writing – review & editing. **Brice Bouyssiere:** Validation. **Emilien Girot:** Investigation. **Jean-François Portha:** Writing – review & editing, Investigation. **Peter Pratt:** Validation. **Lucie Coniglio:** Writing – review & editing, Supervision, Methodology, Conceptualization.

Declaration of competing interest

The authors declare that they have no known competing financial interests or personal relationships that could have appeared to influence the work reported in this paper.

Data availability

Data will be made available on request.

Acknowledgments

The authors are very appreciative to Frédéric Roze, Maud Lebrun, Steve Pontvianne, Philippe Arnoux, and Jean-Marc Commenge for their technical support and helpful discussions during the work (members of Université de Lorraine - Ecole Nationale Supérieure des Industries Chimiques de Nancy, Laboratoire Réactions et Génie des Procédés UMR CNRS 7274, 54001 Nancy Cedex, France).

Appendix

Table A0.1
Analysis equipment and operating conditions regarding to the production, purification and characterization of biodiesel and biolubricant carried out in this work. Partly adapted from Muhammad et al. (2017), Chen et al. (2019), and Roze et al. (2021).

Objective	Technique	Equipment	Operating conditions or Standard
Biodiesel & Biolubricant production			
Monitoring of the transesterification with ethanol or 2-ethylhexanol	Off-line GC-FID with preliminary GC-MS	Agilent Technologies (USA	• *Preliminary ester identification:* Please refer to Nitièma-Yefanova et al. (2015). •*Ester quantification*: Please refer to Mohammad et al. (2017) except for the oven temperature program: 60 °C (2 min), 60–200 °C (10 °C/min), 200–240 °C (5 °C/min), 240 °C (7 min for IMSOEEs, 16 min for IMSO2E1HEs). *After centrifugation of the sampling tubes*, 0.1 mL of the organic phase was *poured* in vials prefilled with 1 mL of stock solution, i.e. a mixture of well-known composition in the internal standard selected for FAEE quantification (MHD) with n-heptane. The *response factors of all FAEEs* relatively to MHD were assigned to the value obtained for ethyl oleate (major component of IMSOEEs, Table 1). Regarding biolubricant quantification, the *response factors of all IMSO2E1HEs* were assigned to 1 (commercial standard of 2-ethylhexyl oleate unavailable) while 1-pentanol was selected as internal standard to determine the residual 2-ethylhexanol and potential traces of ethanol. Note that MHD was used instead of methyl nonadecanoate recommended in the European standard EN-14103 because of overlapping with the ethyl linoleate GC peak (Nitièma-Yefanova et al., 2016).

Objective	Technique	Equipment	Operating conditions or Standard
*Biodiesel characterization – **(a)** Composition*			
Glyceride (TGs, DGs, MGs), free glycerin and FAEE contents	GC-FID	Valtris Enterprises (France)	EN-14105, except for FAEEs: EN-14103
Water content	Coulometric Karl Fischer titration	Valtris Enterprises (France)	EN-ISO-12937
Potassium and other elements (Ag, Al, As, B, Ba, Ca, Cd, Co, Cr, Cu, Fe, Hg, K, Li, Mg, Mn, Mo, Na, Ni, P, Pb, Sb, Sr, Ti, V, Zn, Zr) contents	ICP-AES	ARCOS by SPECTRO; *Scott*-type *double*-pass spray *chamber* combined with *cross-flow* nebulizer (Germany)	Please, refer to Nitièma-Yefanova et al. (2015), Pohl et al. (2010), Caumette et al. (2010) and Ruiz et al. (2023)
	ICP-MS	7700s ICP MS detector (Agilent Technologies, Tokyo, Japan) mounted with Nickel cones. ICP MS was used in collision cell mode with He (11 mL min-1). A Scott-type double pass spray chamber was used combined with a meinhard nebulizer.	
*Biodiesel characterization – **(b)** Fuel properties*			
Acid value	Volumetric titration	Valtris Enterprises (France)	EN-14104
Color	Colorimetry	Valtris Enterprises (France)	ASTM-D1544
Density (15 °C)	Oscillating U-tube	Valtris Enterprises (France)	EN-ISO-12185
Viscosity (40 °C)	Capillarity viscometer	Valtris Enterprises (France)	EN-ISO-3104
Flash point	Estimation	–	Vapor-liquid equilibria estimation based on composition in FAEEs (from GC-FID), their molecular structure, and their vapor pressures as pure components (Carareto et al., 2012)
Cloud point	Estimation	–	Correlation based on number of carbon atoms and composition in FAEEs (from GC-FID) (Bolonio et al., 2015)
Pour point	Estimation	–	Correlation based on number of carbon atoms and composition in FAEEs (from GC-FID) (Bolonio et al., 2015)
Cold filter plugging point (°C)	Estimation	–	Correlation based on number of carbon atoms and composition in FAEEs (from GC-FID) (Bolonio et al., 2015)
Higher heating value (MJ/kg)	Estimation	–	Correlation based on composition in FAEEs (from GC-FID) (Hong et al., 2014)
Oxidation stability at 110 °C (hrs.)	Estimation	–	Correlation based on composition in FAEEs (from GC-FID) (Hong et al., 2014)

Objective	Technique	Equipment	Operating conditions
*Biolubricant characterization – **(a)** Composition*			
Contents in esters and 2-ethylhexanol	Off-line GC-FID with preliminary GC-MS	Agilent Technologies (USA)	Please, see above "*Biodiesel & Biolubricant production*" •Preliminary ester identification and •Ester quantification.
Water content	Coulometric Karl Fischer titration	Valtris Enterprises (France)	EN-ISO-12937

(*continued on next page*)

Table A0.1 (*continued*)

Objective	Technique	Equipment	Operating conditions
Potassium and other elements (Ag, Al, As, B, Ba, Ca, Cd, Co, Cr, Cu, Fe, Hg, K, Li, Mg, Mn, Mo, Na, Ni, P, Pb, Sb, Sr, Ti, V, Zn, Zr) contents	ICP-AES	ARCOS by SPECTRO; *Scott*-type *double*-pass spray *chamber* combined with *cross-flow* nebulizer (Germany)	Please, refer to Nitièma-Yefanova et al. (2015), Pohl et al. (2010), Caumette et al. (2010) and Ruiz et al. (2023)
	ICP-MS	iCAP Q ICP-MAS, Thermo Fisher Scientific Inc.	
*Biolubricant characterization – **(b)** Specific functional properties*			
Acid value	Volumetric titration	Valtris Enterprises (France)	ISO-6618
Color	Colorimetry	Valtris Enterprises (France)	ASTM-D1544
Density (20 °C)	Oscillating U-tube	Valtris Enterprises (France)	EN-ISO-12185
Viscosity (40 and 100 °C)	Capillarity viscometer	Valtris Enterprises (France)	EN-ISO-3104**)**

References

Ainembabazi, D., Wang, K., Finn, M., Ridenour, J., Voutchkova-Kostal, A., 2020. Efficient transfer hydrogenation of carbonate salts from glycerol using water-soluble iridium N-heterocyclic carbene catalysts. Green Chem. 22, 6093–6104. https://doi.org/10.1039/d0gc01958e.

Albuquerque, A.A., Ng, F.T.T., Danielski, L., Stragevitch, L., 2020. Phase equilibrium modeling in biodiesel production by reactive distillation. Fuel 271, 117688. https://doi.org/10.1016/j.fuel.2020.117688.

Anwar, Hossain Md, Iqbal, Mohammad Anwar Mohamed, Muhd Julkapli, Nurhidayatullaili, Kong, Pei San, Ching, Juan Joon, Lee, Hwei Voon, 2018. Development of catalyst complexes for upgrading biomass into ester-based biolubricants for automotive applications: a review. RSC Adv. 8, 5559–5577. https://doi.org/10.1039/c7ra11824d.

ASTM D1983-90, 1995. Standard Test Method for Fatty Acid Composition by Gas-Liquid Chromatography of Methyl Esters (Withdrawn 2003). ASTM International, West Conshohocken, PA, 1995.

Baroi, C., Yanful, E.K., Bergougnou, M.A., 2009. Biodiesel production from Jatropha Curcas oil using potassium carbonate as an unsupported catalyst. Int. J. Chem. React. Eng. 7, 1–18. https://doi.org/10.2202/1542-6580.2027.

Bashir, M.A., Wu, S., Zhu, J., Krosuri, A., Khan, M.U., Junior Ndeddy Aka, R., 2022. Recent development of advanced processing technologies for biodiesel production: a critical review. Fuel Process. Technol. 227, 107120 https://doi.org/10.1016/j.fuproc.2021.107120.

Bolonio, D., Llamas, A., Rodríguez-Fernández, J., Al-Lal, A.M., Canoira, L., Lapuerta, M., Gómez, L., 2015. Estimation of cold flow performance and oxidation stability of fatty acid ethyl esters from lipids obtained from Escherichia coli. Energy Fuels 29, 2493–2502. https://doi.org/10.1021/acs.energyfuels.5b00141.

Boz, N., Degirmenbasi, N., Kalyon, D.M., 2013. Transesterification of canola oil to biodiesel using calcium bentonite functioned with K compounds. Appl. Catal. B Environ. 138–139, 236–242. https://doi.org/10.1016/j.apcatb.2013.02.043.

Carareto, N.D.D., Kimura, C.Y.C.S., Oliveira, E.C., Costa, M.C., Meirelles, A.J.A., 2012. Flash points of mixtures containing ethyl or ethylic biodiesel and ethanol. Fuel 96, 319–326. https://doi.org/10.1016/j.fuel.2012.01.025.

Caumette, G., Lienemann, C.P., Merdrignac, I., Bouyssiere, B., Lobinski, R., 2010. Fractionation and speciation of nickel and vanadium in crude oils by size exclusion chromatography-ICP MS and normal phase HPLC-ICP MS. J. Anal. At. Spectrom. 25, 1123–1129. https://doi.org/10.1039/c003455j.

Cerón, A.A., Vilas Boas, R.N., Biaggio, F.C., de Castro, H.F., 2018. Synthesis of biolubricant by transesterification of palm kernel oil with simulated fusel oil: batch and continuous processes. Biomass Bioenergy 119, 166–172. https://doi.org/10.1016/j.biombioe.2018.09.013.

Chan, C.H., Tang, S.W., Mohd, N.K., Lim, W.H., Yeong, S.K., Idris, Z., 2018. Tribological behavior of biolubricant base stocks and additives. Renew. Sustain. Energy Rev. 93, 145–157. https://doi.org/10.1016/j.rser.2018.05.024.

Chen, J., Bian, X., Rapp, G., Lang, J., Montoya, A., Trethowan, R., Bouyssiere, B., Portha, J.-F., Jaubert, J.-N., Peter Pratt, P., Coniglio, L., 2019. From ethyl biodiesel to biolubricants: options for an Indian mustard integrated biorefinery toward a green and circular economy. Ind. Crop. Prod. 137, 597–614. https://doi.org/10.1016/j.indcrop.2019.04.041.

Coniglio, L., 2023. Illustrations of the synergy between thermodynamics and chemical reaction into the triptych “Bioproducts-Bioenergy-Water”. J. Solut. Chem. https://doi.org/10.1007/s10953-023-01305-z.

Coniglio, L., Bennadji, H., Glaude, P.A., Herbinet, O., Billaud, F., 2013. Combustion chemical kinetics of biodiesel and related compounds (methyl and ethyl esters): experiments and modeling Advances and future refinements. Prog. Energy Combust. Sci. 39, 340–382. https://doi.org/10.1016/j.pecs.2013.03.002.

Coniglio, L., Coutinho, J.A.P., Clavier, J.Y., Jolibert, F., Jose, J., Mokbel, I., Pillot, D., Pons, M.N., Sergent, M., Tschamber, V., 2014. Biodiesel via supercritical ethanolysis within a global analysis “feedstocks-conversion-engine” for a sustainable fuel alternative. Prog. Energy Combust. Sci. 43, 1–35. https://doi.org/10.1016/j.pecs.2014.03.001.

de Caro, P., Bandres, M., Urrutigoïty, M., Cecutti, C., Thiebaux-Roux, S., 2019. Recent progress in synthesis of glycerol carbonate and evaluation of its plasticizing properties. Front. Chem. 308, 1–13. https://doi.org/10.3389/fchem.2019.00308.

de Haro, J.C., del Prado Garrido, M., Pérez, Á., Carmona, M., Rodríguez, J.F., 2018. Full conversion of oleic acid to estolides esters, biodiesel and choline carboxylates in three easy steps. J. Clean. Prod. 184, 579–585. https://doi.org/10.1016/j.jclepro.2018.02.190.

Encinar, J.M., Nogoles-Delgado, S., Pinilla, A., 2021. Biolubricant production through double transesterification: reactor design for the implementation of a biorefinery based on rapeseed. Processes 9, 1224. https://doi.org/10.3390/pr9071224.

Habib, N.S.H.A., Yunus, R., Rashid, U., Taufiq-Yap, Y.H., Abidin, Z.Z., Syam, A.M., Irawan, S., 2014. Transesterification reaction for synthesis of palm-based ethylhexyl ester and formulation as base oil for synthetic drilling fluid. J. Oleo Sci. 63, 497–506. https://doi.org/10.5650/jos.ess13220.

Hong, I.K., Jeon, S.G., Lee, S.B., 2014. Prediction of biodiesel fuel properties from fatty acid alkyl ester. J. Ind. Eng. Chem. 20, 2348–2353. https://doi.org/10.1016/j.jiec.2013.10.011.

Kleinaitė, E., Jaška, V., Tvaska, B., Matijošytė, I., 2014. A cleaner approach for biolubricant production using biodiesel as a starting material. J. Clean. Prod. 75, 40–44. https://doi.org/10.1016/j.jclepro.2014.03.077.

Lanfredi, S., Matos, J., da Silva, S.R., Djurado, E., Sadouki, A.S., Chouaih, A., Poon, P.S., González, E.R.P., Nobre, M.A.I., 2020. K- and Cu-doped $CaTiO_3$-based nanostructures hollow spheres as alternative catalysts to produce fatty acid ethyl esters as potential biodiesel. Appl. Catal. B Environ. 272, 118986 https://doi.org/10.1016/j.apcatb.2020.118986.

McNutt, J., He, Q.S., 2016. Development of biolubricants from vegetable oils via chemical modification. J. Ind. Eng. Chem. 36, 1–12. https://doi.org/10.1016/j.jiec.2016.02.008.

Muhammad, F., Oliveira, M.B., Pignat, P., Jaubert, J.-N., Pinho, S.P., Coniglio, L., 2017. Phase equilibrium data and modeling of ethylic biodiesel with application to a non-edible vegetable oil. Fuel 203, 633–641. https://doi.org/10.1016/j.fuel.2017.05.007.

Naser, J., Mjalli, F., Jibril, B., Al-Hatmi, S., Gano, Z., 2013. Potassium carbonate as a salt for Deep eutectic solvents. Int. J. Chem. Eng. Appl 4, 114–118. https://doi.org/10.7763/IJCEA.2013.V4.275.

Navarro-Pineda, F.S., Baz-Rodríguez, S.A., Handler, R., Sacramento-Rivero, J.C., 2016. Advances on the processing of *Jatropha curcas* towards a whole-crop biorefinery. Renew. Sustain. Energy Rev. 54, 247–269. https://doi.org/10.1016/j.rser.2015.10.009.

Nitièma-Yefanova, S., Richard, R., Thiebaud-Roux, S., Bouyssiere, B., Bonzi-Coulibaly, Y. L., Nébié, R.H., Mozet, K., Coniglio, L., 2015. Dry-purification by natural adsorbents of ethyl biodiesels derived from nonedible oils. Energy Fuels 29, 150–159. https://doi.org/10.1021/ef501365u.

Nitièma-Yefanova, S., Coniglio, L., Schneider, R., Nébié, R.H.C., Bonzi-Coulibaly, Y.L., 2016. Ethyl biodiesel production from non-edible oils of *Balanites aegyptiaca, Azadirachta indica*, and *Jatropha curcas* seeds – laboratory scale development. Renew. Energy 96, 881–890. https://doi.org/10.1016/j.renene.2016.04.100.

Nitièma-Yefanova, S., Tschamber, V., Richard, R., Thiebaud-Roux, S., Bouyssiere, B., Bonzi-Coulibaly, Y.L., Nébié, R.H.C., Coniglio, L., 2017. Ethyl biodiesels derived from non-edible oils within the biorefinery concept – pilot scale production & engine emissions. Renew. Energy 109, 634–645. https://doi.org/10.1016/j.renene.2017.03.058.

Pabsch, D., Figiel, P., Sadowski, G., Held, C., 2022. Solubility of electrolytes in organic solvents: solvent-specific effects and ion-specific effects. J. Chem. Eng. Data 67, 2706–2718. https://doi.org/10.1021/acs.jced.2c00203.

Panchal, T.M., Patel, A., Chauhan, D.D., Thomas, M., Patel, J.V., 2017. A methodological review on bio-lubricants from vegetable oil-based resources. Renew. Sustain. Energy Rev. 70, 65–70. https://doi.org/10.1016/j.rser.2016.11.105.

Pawar, R.V., Hulwan, D.B., Mandale, M.B., 2022. Recent advancements in synthesis, rheological characterization, and tribological performance of vegetable oil-based lubricants enhanced with nanoparticles for sustainable lubrication. J. Clean. Prod. 378, 134454 https://doi.org/10.1016/j.jclepro.2022.134454.

Pedro, K.C.N.R., Ferreira, I.E.P., Henriques, C.A., Langone, M.A.P., 2020. Enzymatic fatty acid ethyl esters synthesis using acid soybean oil and liquid lipase formulation. Chem. Eng. Commun. 207, 43–55. https://doi.org/10.1080/00986445.2019.1572001.

Pohl, P., Vorapalawut, N., Bouyssiere, B., Carrier, H., Lobinski, R., 2010. Direct multi-element analysis of crude oils and gas condensates by double-focusing sector field inductively coupled plasma mass spectrometry (ICP MS). J. Anal. At. Spectrom. 25, 704–709. https://doi.org/10.1039/c000658k.

Raman, J.K., Alves, C.M., Gnansounou, E., 2018. A review on moringa tree and vetiver grass - potential biorefinery feedstocks. Bioresour. Technol. 249, 1044–1051. https://doi.org/10.1016/j.biortech.2017.10.094.

Rapp, G., 2018. The Value of Indian Mustard in Cereal and Legume Crop Sequences in Northwest NSW. University of Sydney, Australia. Master Thesis. http://hdl.handle.net/2123/18504.

Rapp, G., Garcia-Montoto, V., Bouyssiere, B., Thiebaud-Roux, S., Montoya, A., Trethowan, R., Pratt, P., Mozet, K., Coniglio, L., 2020. Dry-purification by natural adsorbents of Indian mustard seed oil ethyl biodiesel and biolubricants: toward a low-cost and environmentally-friendly production route. In: 28th European Biomass Conference and Exhibition Proceedings, pp. 621–624.

Rapp, G., Garcia-Montoto, V., Bouyssiere, B., Thiebaud-Roux, S., Montoya, A., Trethowan, R., Pratt, P., Mozet, K., Portha, J.F., Coniglio, L., 2021. Indian mustard bioproducts dry-purification with natural adsorbents – a biorefinery for green circular economy. J. Clean. Prod. 286, 125411 https://doi.org/10.1016/j.jclepro.2020.125411.

Reeves, C.J., Menezes, P.L., Jen, T.C., Lovell, M.R., 2015. The influence of fatty acids on tribological and thermal properties of natural oils as sustainable biolubricants. Tribol. Int. 90, 123–134. https://doi.org/10.1016/j.triboint.2015.04.021.

Roy, P., Rahman, T., Jackson, R.L., Jahromi, H., Adhikari, S., 2023. Hydrocarbon biolubricants from hydrotreated renewable and waste derived liquid intermediates. J. Clean. Prod. 409, 137120 https://doi.org/10.1016/j.jclepro.2023.137120.

Roze, F., Pignat, P., Ferreira, O., Pinho, S.P., Jaubert, J.N., Coniglio, L., 2021. Phase equilibria of mixtures involving fatty acid ethyl esters and fat alcohols between 4 and 27 kPa for bioproduct production. Fuel 306, 121304. https://doi.org/10.1016/j.fuel.2021.121304.

Ruiz, W., Guillemant, J., Coniglio, L., Rodgers, R.P., Christensen, J.H., Garcia-Montoto, V., Verdier, S., Giusti, P., Barrère-Mangote, Bouyssiere, C., 2023. Bio-oil inorganic analysis: a minireview of current trends, challenges, and future perspectives. Energy Fuels 37, 11608–11621. https://doi.org/10.1021/acs.energyfuels.3c01462.

Sarker, M.I., Sharma, B.K., Ngo, H., Muir, Z., Jones, K.C., 2023. Green Synthesis and property analysis of biolubricants based on structural variations. ACS Sustain. Chem. Eng. 11, 11281–11293. https://doi.org/10.1021/acssuschemeng.3c02996.

Schick, D., Arrad, M., Figiel, P., Sadowski, G., Held, C., 2023. Modeling the temperature-dependent solubility of salts in organic solvents. Fluid Phase Equil. 572, 113828 https://doi.org/10.1016/j.fluid.2023.113828.

Sejati, P.S., Akong, F.O., Torloting, C., Fradet, F., Gérardin, P., 2023. Thermoplastic translucent film from wood and fatty acids by solvent free esterification: influence of fatty acid chain length. Eur. Polym. J. 196, 112276 https://doi.org/10.1016/j.eurpolymj.2023.112276.

Sharma, B.K., Biresaw, G., 2016. Environmentally Friendly and Biobased Lubricants, first ed. CRC Press Taylor & Francis Group. ISBN 9781482232028.

Silveira Junior, E.G., Perez, V.H., Reyero, I., Serrano-Lotina, A., Justo, O.R., 2019. Biodiesel production from heterogeneous catalysts based K_2CO_3 supported on extruded γ-Al_2O_3. Fuel 241, 311–318. https://doi.org/10.1016/j.fuel.2018.12.074.

Singh, V.V., Garg, P., Meena, H.S., Meena, M.L., 2018. Drought stress response of Indian mustard (*Brassica juncea L.*) genotypes. Int. J. Curr. Microbiol. App. Sci. 7, 2519–2526. https://doi.org/10.20546/ijcmas.2018.703.291.

Sun, G., Li, Y., Cai, Z., Teng, Y., Wang, Y., Reaney, M.J.T., 2017. K_2CO_3-loaded hydrotalcite: a promising heterogeneous solid base catalyst for biolubricant base oil production from waste cooking oils. Appl. Catal. B Environ. 209, 118–127. https://doi.org/10.1016/j.apcatb.2017.02.078.

Syahir, A.Z., Zulkifli, N.W.M., Masjuki, H.H., Kalam, M.A., Alabdulkarem, A., Gulzar, M., Khuong, L.S., Harith, M.H., 2017. A review on bio-based lubricants and their applications. J. Clean. Prod. 168, 997–1016. https://doi.org/10.1016/j.jclepro.2017.09.106.

Turkkul, B., Deliismail, O., Seker, E., 2020. Ethyl esters biodiesel production from Spirulina sp. and Nannochloropsis oculata microalgal lipids over alumina-calcium oxide catalyst. Renew. Energy 145, 1014–1019. https://doi.org/10.1016/j.renene.2019.06.093.

Ubando, A.T., Felix, C.B., Chen, W.S., 2020. Biorefineries in circular bioeconomy: a comprehensive review. Bioresour. Technol. 299, 122585 https://doi.org/10.1016/j.biortech.2019.122585.

Valtris Enterprises France, Verdun, France, 2023. Private Communication.

Zheng, T., Wu, Z., Xie, Q., Lu, M., Xia, F., Wang, G., Nie, Y., Ji, J., 2018. Biolubricant production of 2-ethylhexyl palmitate by transesterification over unsupported potassium carbonate. J. Am. Oil Chem. Soc. 95, 79–88. https://doi.org/10.1002/aocs.12023.